Original article

The Effect of Dust Aerosol on Satellite Data from Different Color Scanners

A. S. Papkova, E. B. Shybanov ✉, D. V. Kalinskaya

Marine Hydrophysical Institute of RAS, Sevastopol, Russian Federation
✉ *e-shybanov@mail.ru*

Abstract

Purpose. The work is purposed at evaluating the errors in atmospheric correction of the satellite (*MODIS Aqua*, *MODIS Terra*, *VIIRS SNPP, VIIRS JPSS, NASA HawkEye* (*SeaHawk*) and *OLCI* (*Sentinel 3A*)) data for July 28–29, 2021 when a dust transport over the Black Sea region was recorded. *Methods and Results*. To assess the scale and intensity of the studied dust transfer, the results of *in situ* photometric measurements and satellite data were analyzed. The *in situ* measurement data on aerosol optical depth (AOD) were obtained at the western Black Sea stations *Galata_Platform* and *Section_7* of the *AERONET* network (*AErosol RObotic NETwork*). The variability of sea remote sensing reflectance values during the period under study was analyzed using the additional *AERONET − Ocean Color* (*AERONET-OC*) data. The color scanner (*MODIS Aqua/Terra, VIIRS SNPP/JPSS, HawkEye* and *OCLI*) measurements presented in the *Ocean Color* database were used as satellite data.

Conclusions. The approximation of errors in atmospheric correction of satellite data for July 28–29, 2021 has resulted in obtaining the power-law dependencies close to λ^{-5}. This is explained by the total contribution of molecular component (λ^{-4}) and aerosol absorption (λ^{-1}). On July 29, 2021, a better pronounced power function is observed since the dust aerosol concentration increases on this day, whereas the contribution of aerosol absorption becomes close to the power dependence λ^{-2}. Also on the same day, the *CALIPSO* satellite data showed the presence of not only dust aerosol, but also the biomass burning over the region under study. Modeling the back trajectories of *HYSPLIT* air flows has shown that just on this day the aerosol masses moved towards the Black Sea from the southwest (Crete Island), that was additionally confirmed by high AOD values over the eastern Mediterranean Sea on July 29, 2021. The combination of two types of absorbing aerosols is assumed to induce even larger inaccuracies in determining the sea remote sensing reflectance for the period under study.

Keywords: *MODIS, VIIRS, HawkEye, Sentinel, SPM, AERONET, CALIPSO, HYSPLIT* back trajectories, dust aerosol, biomass burning, sea remote sensing reflectance, aerosol optical depth, AOD*,* absorption, Black Sea, atmospheric aerosol, satellite monitoring, ground monitoring, optical characteristics

For citation: Papkova, A.S., Shybanov, E.B. and Kalinskaya, D.V., 2024. The Effect of Dust Aerosol on Satellite Data from Different Color Scanners. *Physical Oceanography*, 31(5), pp. 720-735.

© 2024, A. S. Papkova, E. B. Shybanov, D. V. Kalinskaya

© 2024, Physical Oceanography

Introduction

Mineral dust is often neglected in the analysis of anthropogenic climate change, as it is considered part of the natural aerosol. Some researchers believe that dust may be an important climate-forming component, especially over certain oceanic areas and regions where its concentrations are high [1, 2]. Although it is impossible to determine the exact impact of mineral dust on the global climate, research on this topic is interdisciplinary and relevant. Complete information on the properties of different types of aerosols (including absorbing aerosols) can be obtained by comprehensive determination of their concentration, microstructure, chemical composition and optical properties [3−5].

This study is a continuation of a series of works dedicated to the examination of optical properties of the dust aerosol over the Black Sea and its influence on *Ocean Color* products. For the region under study, the results obtained when analyzing satellite data can in many cases have large errors due to incorrect consideration of the optical properties of the aerosol [6−9]. It is worth noting that dust transports from both the African continent as well as from the Middle East and Asia are observed annually over the Black Sea region [10]. Since the MHI RAS scientists have been studying this topic for more than 10 years, there is already a certain method to identify different types of aerosols (background aerosol, smoke and dust) based on the variability of optical properties, such as aerosol optical depth (AOD), Angstrom parameter (α), single scattering albedo (SSA), size distribution and concentration of aerosol particles (fine (*PM*2.5) and coarse (*PM*10) particles), asymmetry parameter, etc. The dust aerosol identification method combines a visual analysis of satellite images, which clearly show a dust plume, and an analysis of photometric measurements of the optical properties of the aerosol. To analyze the aerosol over the Black Sea region, data from the *AERONET* network stations (*Galata_Platform, Section_7*) located in the western part of the Black Sea are used, as well as unique data from the portable SPM spectrophotometer and the ATMAS dust meter, which were measured daily on the MHI RAS territory [11−13].

It is worth noting that dust aerosol has the greatest impact not only on the variability of the optical properties of the atmosphere, but also on the *Ocean Color* satellite products. For an objective assessment of the state of the water surface and the procedure for atmospheric correction based on remote sensing data, it is necessary to carry out a comparative analysis of three types of measurement data: satellite, model and *in situ*. In [8, 14−28], it is shown that in the presence of dust, the sea remote sensing reflectance can have negative values in the shortwave range (400−443 nm). This fact indicates systematic errors in the operation of standard atmospheric correction algorithms, which are based on the principle of extrapolating aerosol properties from the near-IR part of the spectrum to the visible part [27]. In a previous work [18], it was shown analytically that in the presence of dust-absorbing aerosol in the atmosphere

above the region, the error in the atmospheric correction is expressed by a fourth-degree power function, i.e. it is close to λ^{-4}. This is due to the absorption by the aerosol of radiation scattered by the air molecules. The analytical expression describing the dependence of the error value of the standard atmospheric correction on the aerosol stratification, for small values of the optical depth of light absorption by the aerosol $a_0(\lambda)$, has the following form

$$r = \frac{p_m(\cos\gamma)\cdot\tau_m^0(\lambda)}{4\mu_0\mu}\,a_0(\lambda)\cdot\left(\frac{1}{\mu_0}+\frac{1}{\mu}\right)\int\limits_0^1\int\limits_0^p g(x)dx\cdot dp\,, \qquad (1)$$

$$a_0(\lambda) = (1-\Lambda)\tau_a^0,$$

where τ_a^0 is the aerosol optical depth; Λ is the single scattering albedo; μ_0 is the cosine of the solar zenith angle; μ is the cosine of the observation zenith angle; $\cos\gamma = -\mu_1\cdot\mu_2+\sqrt{1-\mu_1^2}\sqrt{1-\mu_2^2}\cos\varphi$ is the cosine of the scattering angle; τ_m^0 is the total optical depth of the molecular atmosphere; $g(x)$ is the dust aerosol stratification function, which shows the dependence of the relative concentration of aerosol particles on atmospheric pressure at a given altitude. The first fraction in expression (1) is nothing more than the expression for the sensing reflectance of the molecular atmosphere in the linear Gordon approximation. Consequently, three factors can be identified that influence the magnitude of the atmospheric correction error. The multiplier $\frac{p_m(\cos\gamma)}{\mu_0\mu}\left(\frac{1}{\mu_0}+\frac{1}{\mu}\right)$ describes the observation geometry, and the double integral is independent of the wavelength and takes into account stratification of the absorbing aerosol relative to the air molecules. Consequently, the spectral properties of the atmospheric correction error are described by the factors $\tau_m^0(\lambda)$ and a_0. It is known that, according to the Rayleigh law, $\tau_m^0 \approx \lambda^{-4}$, spectral properties of aerosol absorption are determined by aerosol microphysics, which for dust aerosol depends on the dust sources and their transformation processes in the atmosphere. Until now, the spectral dependence variability a_0 has not been considered. In this paper, it is proposed to estimate for the first time the spectral behavior of the absorption properties of dust aerosol for the case of dust transfer over the Black Sea region.

Experimental regularities of the atmospheric correction error were analyzed in [18]. It was shown that the largest difference between satellite and *in situ* remotely sensed ocean reflectance data is recorded in the presence of dust aerosol in the atmosphere. For the selected 49 data obtained on dust transfer days, the principal component method with the first vector contribution estimation was used. The result showed that 86% of the variance of the *MODIS-Aqua* validation error is explained

by the first eigenvector, which is well approximated by a power law $\lambda^{-3.57\pm0.32}$. This confirmed the reliability of the analytical estimates [18].

The objective of this study is to estimate the magnitude of the atmospheric correction error of *MODIS-Aqua*, *MODIS-Terra*, *VIIRS-SNPP*, *VIIRS-JPSS*, *NASA HawkEye (SeaHawk)* and *OLCI-Sentinel-3A* satellite data for 28–29 July 2021, when dust transport over the Black Sea region was recorded.

The present study focuses on an analysis of the variability of the optical properties of the atmosphere on 28–29 July 2021 over the Black Sea region and the evidence (based on satellite and model data) that it is dust aerosol that is recorded over the region during the period under consideration.

The second stage is dedicated to the estimation of the impact of the absorbing dust aerosol on the size of the atmospheric correction error in the calculation of the sea remote sensing reflectance for 28 and 29 July 2021. For these dates, the largest number of different satellite measurements, synchronized with *in-situ* remote sensing sea reflectance measurements according to the *AERONET – Ocean Color (AERONET-OC)* network, were obtained. In this study, the validation error was calculated for *MODIS-Aqua/Terra, VIIRS-JPSS, Sentinel-3A* and *HawkEye (SeaHawk)*.

Instruments and materials

The photometric data from the international *AERONET (Aerosol ROboties NETwork)* were used as a source for the *in-situ* AOD measurements. The data from the *AERONET-OC* extension, which allow the measurement of radiation from underwater, were used to analyze the sea remote sensing reflectance data [29]. Currently, two stations, Black Sea *Section_7* (29.45°E, 44.45°N) and *Galata_Platform* (28.19°E, 43.05°N), provide information on seawater color. In this paper, an array of daily mean data on normalized L_{WN} level 2 (higher quality) water radiation has been analyzed. The level 1.5 data array is selected taking into account cloudiness through a series of quality tests, and the level 2 data array consists of fully cleaned data obtained after calibration and software verification. During the studies, $L_{WN}(\lambda)$ values were converted to $R_{rs}(\lambda)$ values by dividing by the solar constant Fo(λ) [30].

To compare satellite and *in situ* measurements for 28–29 July 2021 and to correct for inaccuracies caused by variability and anomalies in atmospheric parameters, the data from the international *AERONET* photometer network, freely available at http://aeronet.gsfc.nasa.gov and the *MODIS-Aqua/Terra*, *VIIRS-SNPP/JPSS*, *HawkEye* and *OCLI* data, freely available at https://Ocean Color.gsfc.nasa.gov, were selected. The *MODIS* optical properties data are the result of a combination of *Terra* and *Aqua* satellite measurements, providing near real-time information. The resolution of the *MODIS* sensor is 0.5°, the resolution of the images is 2 km, and the temporal resolution is diurnal.

A complicating factor in the study is that the wavelengths at which the *AERONET-OC* station measurements are provided do not fully match

the channels measured by the satellites, especially in the visible range. Thus, the *MODIS-Aqua/Terra* measurement channels have wavelengths of 412, 443, 469, 488, 531, 547, 555, 667 and 678 nm; *VIIRS-JPSS* − wavelengths of 411, 445, 489, 556 and 667 nm. For *HawkEye*, $R_{rs}(\lambda)$ are measured at wavelengths of 412, 488, 510, 556 and 670 nm. The problem of interpolating the sea remote sensing reflectance values obtained in the *CIMEL*-318 photometer channels to the satellite channels is due to the complex shape of the seawater absorption spectrum. Scattering also affects the shape of $R_{rs}(\lambda)$. However, the corresponding spectral dependencies are monotonous and smoother, allowing the use of a second-degree polynomial in the interpolation. In the absorption spectrum, special attention is paid to the absorption of pure seawater, since it greatly affects the variability of the $R_{rs}(\lambda)$ values in the long wavelength region of the spectrum. The absorption spectrum of pure seawater introduces the largest interpolation errors.

In this study, a method was used which consists of multiplying the sea remote sensing reflectance obtained from field measurements by the seawater model absorption value:

$$a_w(\lambda_i) = a_{pw}(\lambda_i) + 0.1 \cdot C_y \cdot exp[0.015 \cdot (400 - \lambda_i)], \qquad (2)$$

where C_y is estimated by statistical relationship with color index:

$$C_y = 2.3 \cdot CI(555/510)^{2.18}. \qquad (3)$$

Expression (3) was obtained based on the regression dependencies given in [31]. After multiplying the natural sea remote sensing reflectance by the model absorption, a second-degree polynomial interpolation was applied to the satellite channels. The resulting values were then divided by the model absorption value at the satellite wavelengths.

The data from the *CALIPSO* satellite were analyzed to determine the predominant aerosol type during the study period. This is an American-French research satellite launched as part of *NASA EOS (Earth Observing System)* program to study the Earth's cloud cover and the vertical structure of atmospheric aerosol. Its main instrument is a three-channel imaging radiometer (8.65, 10.6 and 12.05 mkm). Aerosol types are determined by the value of the integrated backscattering coefficient and the particle depolarization coefficient. The aerosol types determined by the calculations of the *CALIPSO* algorithms are: smoke (from forest fires), dust, contaminated dust (mixtures of dust and smoke), contaminated continental and clean continental aerosol [32]. Each aerosol type is characterized by a set of lidar ratios at the 532 and 1064 nm wavelengths [33].

To obtain information on the source of the smoke aerosols, the results of the calculation of reverse trajectories of air mass transfer, obtained using the *HYSPLIT* modeling software package, were used. Reverse trajectory analysis

makes it possible to follow the movement of air flows at different altitudes and to identify the location of likely sources of pollution entering the atmosphere [34].

Results and discussion

On 28–29 July 2021, satellite data showed intense dust transport from the Arabian Peninsula and the Sahara across the Black Sea region. According to the *VIIRS* false-color satellite images, dust transport is recorded on both sides of the illuminated area, which means that the size of the dust event is more than a thousand square kilometers. All presented satellite images also clearly show the area of intense fires on the Mediterranean coast (territory of Turkey). Intense absorption due to the presence of smoke aerosol west of the island of Crete is confirmed by high AOD values over the eastern part of the Mediterranean Sea on 29 July 2021 (Fig. 1). The next step is confirming or refuting of the dust transfer event over the Black Sea region during the study period was the analysis of the reverse trajectories of the air flow movement using the *HYSPLIT* model [34] (Fig. 1, *b*, *d*). As shown in Fig. 1, dust transfer from the Sahara was recorded at the 3 km level for all days.

T a b l e 1

Optical characteristics of atmospheric aerosol over the *AERONET-OC* stations in the Black Sea

Aerosol parameters	Section-7_Platform			Galata_Platform		
	27.07.2021	28.07.2021	29.07.2021	27.07.2021	28.07.2021	29.07.2021
AOD_1020nm	0.1044	0.1594	0.15640	0.118754	0.153976	0.145702
AOD_865nm	0.1184	0.1774	0.17599	0.133570	0.169755	0.164323
AOD_779nm	0.1273	0.1888	0.18826	0.142891	0.179414	0.177168
AOD_667nm	0.1510	0.2150	0.21895	0.163671	0.200484	0.205612
AOD_620nm	0.1640	0.2299	0.23420	0.175332	0.211100	0.220486
AOD_560nm	0.1859	0.2543	0.26190	0.194556	0.230445	0.247066
AOD_510nm	0.2079	0.2793	0.29050	0.214621	0.251795	0.276285
AOD_490nm	0.2163	0.2880	0.30092	0.222911	0.259967	0.287855
AOD_443nm	0.2425	0.3173	0.33410	0.247029	0.284315	0.322171
AOD_412nm	0.2667	0.3432	0.36280	0.266241	0.303928	0.349083
AOD_400nm	0.2801	0.3569	0.37790	0.275084	0.313003	0.361403
α(440-870)	1.1110	0.8871	0.98910	0.979185	0.782825	1.027634
α(440-675)	1.1687	0.9532	1.06210	1.051961	0.867812	1.117899

In this paper, a comparative analysis of the aerosol optical properties at *AERONET* stations (*Galata_Platform* and *Section_7_Platform*) was performed for cases of different aerosol activity, namely: for 28 July 2021 (the day of the intense dust transfer), 27 July 2021 (the day before the dust transfer in the presence of

background aerosol) and 29 July 2021 (the day after the start of the intense dust transfer). It is worth noting that in July 2021 cloudiness was often observed over the *AERONET* stations and therefore the initial monthly mean AOD values were overestimated, which is typical for summer months [35] (Table 1).
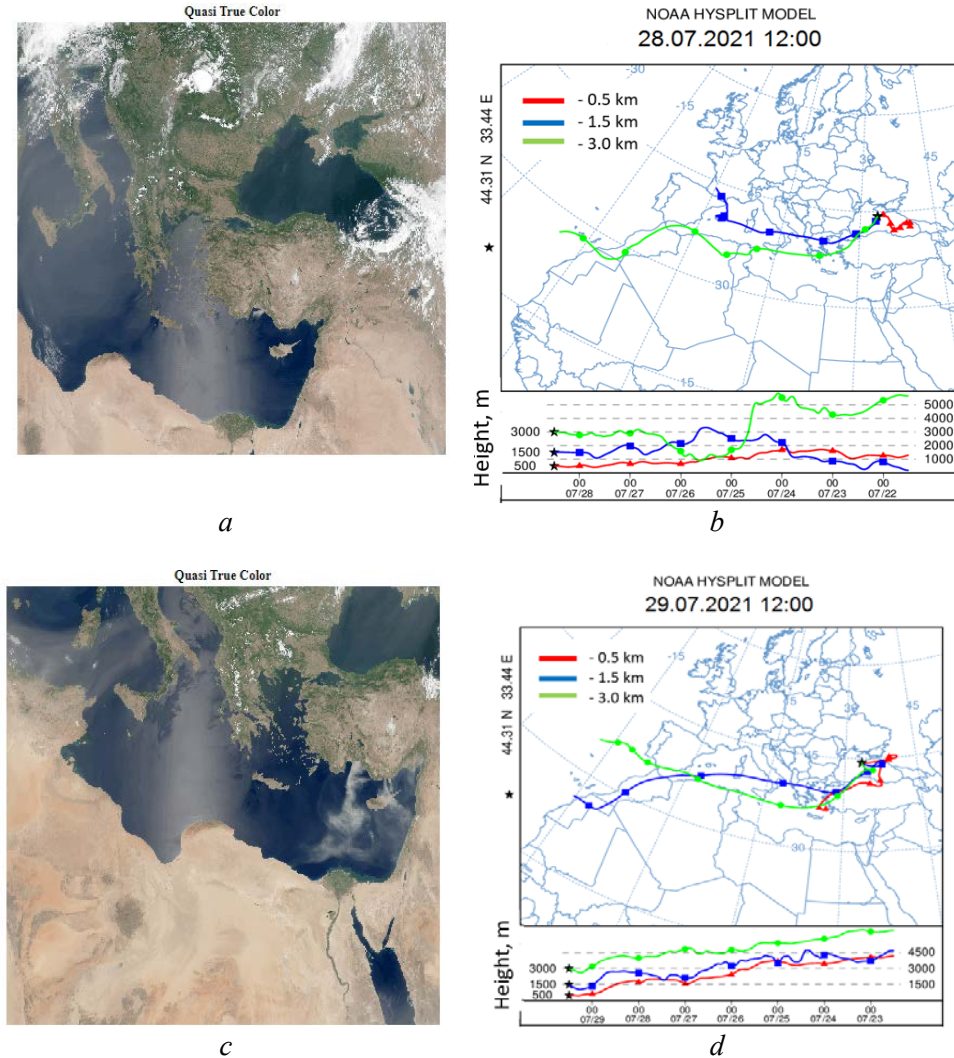
F i g. 1. Satellite images of *VIIRS-SNPP/JPSS* from 28 July 2021 (*a*) and 29 July 2021 (*c*) (source: https://oceancolor.gsfc.nasa.gov), and corresponding *HYSPLIT* back trajectories (*b*, *d*) (source: https://www.ready.noaa.gov/HYSPLIT_traj.php)

At both western *AERONET* stations in the Black Sea region, a large amount (compared to background values) of coarse aerosol fraction (more than 2.5 μm) and low (SSA < 1) values of the single scattering albedo (SSA) were observed on 28 July 2021 (Fig. 2). In general, a similar situation was observed on 29 July 2021, except for higher values of the Angstrom parameter.

F i g. 2. At the *AERONET* network stations on 28 July 2021: contribution of fine (less than 2.5 mkm) and coarse particles (2.5 mkm and more) to the overall distribution of AOD at *Galata_Platform* (*a*) and *Section_7* (*c*), single scattering albedo at *Galata_Platform* (*b*) and *Section_7* (*d*), particle size distribution at two stations (*e*)

For the first time, an estimate of the optical depth of aerosol absorption is given for the general assessment of the absorption properties of dust aerosol:

$$a_0(\lambda) = (1 - \Lambda(\lambda))\tau_a^0(\lambda). \tag{4}$$

Consequently, the average daily variation of the power function of the optical absorption depth was analyzed for synchronous pairs of AOD and SSA measurements for *AERONET* stations (Fig. 3).
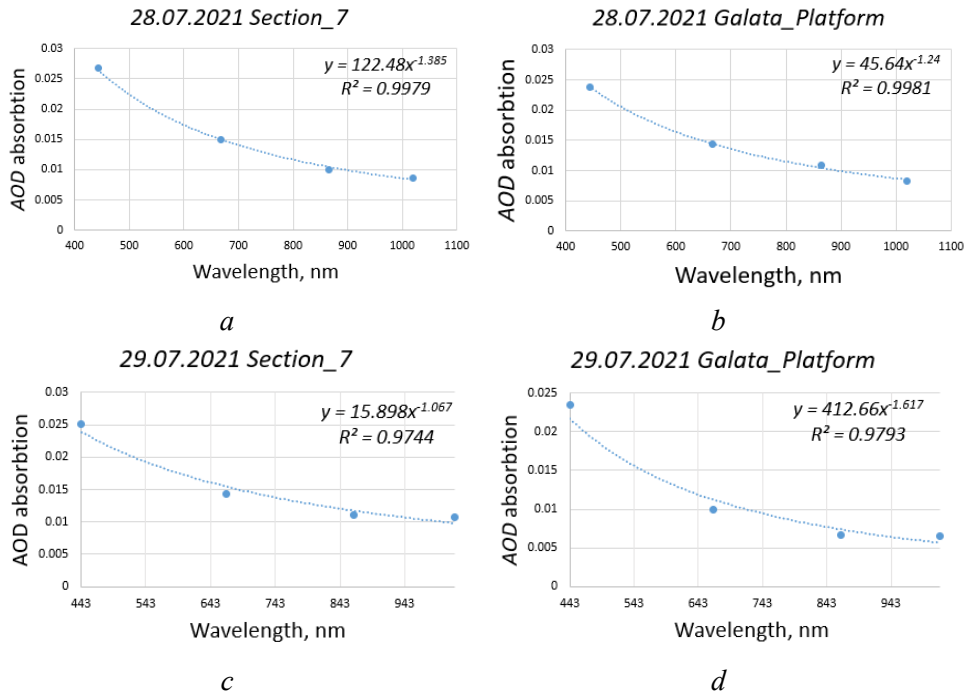
F i g. 3. Mode of the power function of aerosol absorption optical depth at *Galata_Platform* (*a*) and *Section_*7 (*b*) for 28 July 2021, and at *Galata_Platform* (*c*) and *Section_*7 (*d*) for 29 July 2021

From Fig. 3 it is evident that the power function is close to λ^{-1}. Consequently, the magnitude of the atmospheric correction error depends not only on the λ^{-4} factor, but also on the light absorption by the aerosol. As a result, the error of the standard atmospheric correction will increase at shorter wavelengths. It should be noted that the standard atmospheric correction procedure is not capable of qualitatively estimating the change in spectral properties of aerosol scattering under the influence of light absorption in the near IR region, due to the smallness of this effect in the long wavelength part of the spectrum. For this reason, it is necessary to use additional information about the optical properties of the underlying surface in the shortwave region. Thus, the application of standard algorithms for atmospheric correction of satellite data in the presence of absorbing dust aerosol requires an additional regional correction. The product $a_0(\lambda)\cdot\lambda^{-4}$ should be used as the interpolation function, and the proportionality coefficient is found from the conditions imposed on the sea remote sensing reflectance in the shortwave region of the spectrum.

The next stage of the study is to calculate the atmospheric correction error for the *MODIS-Aqua/Terra, VIIRS-SNPP/JPSS, HawkEye* and *Sentinel-3*A satellites for the dates considered. The validation procedure for the satellite data was similar to that used for the *SeaBASS* database: synchronous pairs of measurements with the smallest time difference within a radius of 5 km around the western Black Sea *AERONET-OC* stations were selected. Using the *SeaDAS* software package, all pixels with the following error flags were similarly excluded: *LAND, STRAYLIGHT, HIGLINT, HILT, MODGLINTATMWAR* and *NAVFAILE* [36]. Unfortunately, the *VIIRSS-SNPP* satellite data for 28 July 2021 were excluded from further analysis

because all pixels within a 5 km radius of the *AERONET-OC* stations were within the satellite illumination zone. The synchronous *in situ* measurements of Rrs(λ) at the *AERONET-OC* stations in the western Black Sea during the day changed little, namely: the standard deviation (SD) was less than 10% of the value, allowing the use of daily averages. The interpolation results constructed from the results of sea remote sensing reflectance measurements by *MODIS-Aqua, VIIRS-JPSS, Hawkeye* and *OCLI Sentinel-3*A satellites for 28 July 2021 are shown in Fig. 4.
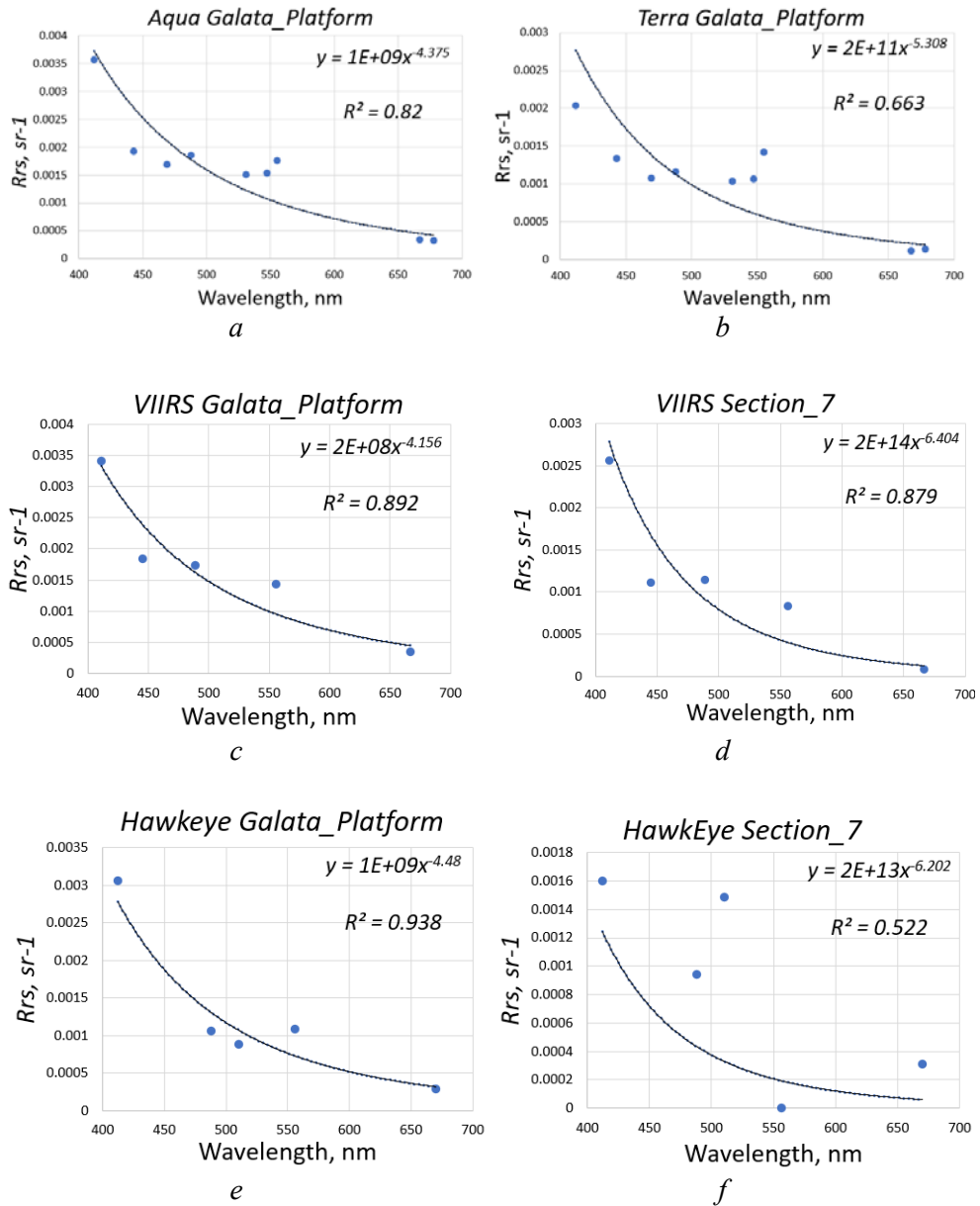
F i g. 4. Errors of atmospheric correction and their approximation by power dependence for 28 July 2021

The atmospheric correction error was similarly calculated for 29 July 2021, when the dust aerosol AOD was higher, but the Ångström parameter was lower (Fig. 5). Unfortunately, the *Modis-Terra* and *VIIRS-SNPP* data had strong outliers and after filtering the error flags, there were no data left.

a

b

c

d

e

f
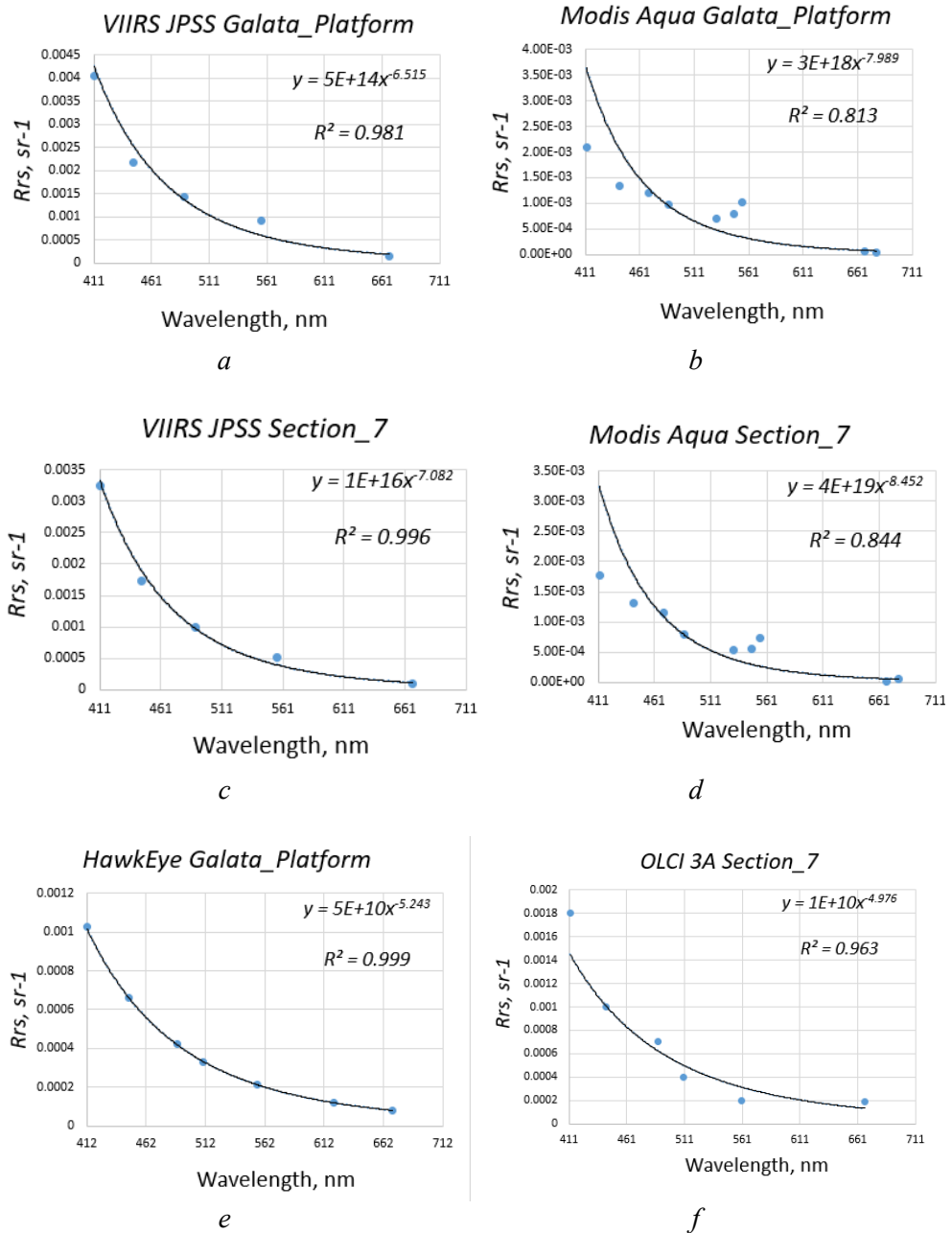
F i g. 5. Errors of atmospheric correction based on the results of measurements of sea remote sensing reflectance by satellites *MODIS-Aqua*, *VIIRS-JPSS*, *Hawkeye* and *OCLI Sentinel* 3*A* for the Black Sea *AERONET-OC* stations for 29 July 2021

As a result of approximation of the atmospheric correction errors for 28 July 2021, power-law dependencies close to λ^{-5} were obtained. This is explained by the total contribution of: 1) the molecular component (λ^{-4}) and 2) the aerosol absorption (λ^{-1}). Fig. 4 shows that the atmospheric correction error of the sea remote sensing reflectance for the *Galata_Platform* station, obtained from *VIIRS-JPSS* and *HawkEye* measurements, is close to the power-law dependence $\lambda^{-4} - \lambda^{-5}$, and for the *Section_7* station it has a more pronounced power-law dependence, namely λ^{-7}. A pronounced shape of the power-law function is observed on 29 July 2021, when the dust aerosol concentration increases and its aerosol absorption is already close to λ^{-2}. It is worth noting that the largest atmospheric correction errors were found for 29 July 2021 according to *MODIS-Aqua* data, whose interpolation function is close to the form λ^{-8}. We believe that this is due to underestimated R_{rs} measurements in the longwave region for this day and consequently large errors in the standard power law approximation – the logarithmic method followed by linear optimization. Using a nonlinear approximation, the power function was obtained in the form $\lambda^{-4} - \lambda^{-5}$, which also indicates large errors in the shortwave region of the spectrum. The maximum errors in the blue region are observed in Fig. 4, *a*, *c*; 5, *a*, *c*.

It is worth noting that the new *HawkEye* and *Sentinel-3*A satellites, despite their short lifetime and a low number of reprocessings and calibrations, show more accurate results. This may be due to the better spatial resolution of the new satellite instruments.

Analysis of *CALIPSO* satellite data on the stratification of different aerosol types for 28 and 29 July 2021 confirmed the presence of dust particles in the surface atmospheric column up to 5 km over the Black Sea. In addition to dust aerosol, contaminated dust and smoke aerosol were recorded on 29 July 2021, which also confirms the spatial distribution of smoke towards The Black Sea region shown in Fig. 1, *c*.

Conclusion

As a result of the approximation of the atmospheric correction errors of the satellite data for 28 July 2021, power-law dependencies close to λ^{-5} were obtained. This is explained by the total contribution of the molecular component (λ^{-4}) and the aerosol absorption (λ^{-1}). For 29 July 2021, a pronounced power-law behavior is observed as the dust aerosol concentration increases and the contribution of aerosol absorption becomes close to the λ^{-2} power-law dependence. In addition, for 29 July 2021, the presence of both dust and smoke aerosols was shown over the study region according to *CALIPSO* satellite data. According to the *HYSPLIT* air flow backtracking modeling data, the aerosol masses on this day moved from the southwest (Crete) towards the Black Sea, which is further confirmed by the high AOD values over the eastern Mediterranean on 29 July 2021. It is assumed that the combination of two absorbing aerosol types caused even greater inaccuracies in the determination of the spectral sea remote sensing reflectance for the period under study.

REFERENCES

1. Koren, I., Kaufman, Y.J., Washington, R., Todd, M.C., Rudich, Y., Martins, J.V. and Rosenfeld, D., 2006. The Bodele Depression: A Single Spot in the Sahara that Provides Most of the Mineral Dust to the Amazon Forest. *Environmental Research Letters*, 1(1), 014005. https://doi.org/10.1088/1748-9326/1/1/014005

2. Kubilay, N., Cokacar, T. and Oguz, T., 2003. Optical Properties of Mineral Dust Outbreaks over the Northeastern Mediterranean. *Journal of Geophysical Research: Atmospheres*, 108(D21), 4666. https://doi.org/10.1029/2003JD003798

3. Suslin, V.V., Slabakova, V.K., Kalinskaya, D.V., Pryakhina, S.F. and Golovko, N.I., 2016. Optical Features of the Black Sea Aerosol and the Sea Water Upper Layer Based on In Situ and Satellite Measurements. *Physical Oceanography*, (1), pp. 20-32. https://doi.org/10.22449/1573-160X-2016-1-20-32

4. Suslin, V.V. and Churilova, T.Ya., 2010. Simplified Method of Calculation of Spectral Diffuse Beam Attenuation Coefficient in the Black Sea Upper Layer on the Basis of Satellite Data. In: MHI, 2010. *Ecological Safety of Coastal and Shelf Zones and Comprehensive Use of Shelf Resources*. Sevastopol: ECOSI-Gidrofizika. Iss. 22, pp. 47-60 (in Russian).

5. Glukhovets, D., Salyuk, P., Sheberstov, C., Vazyulya, S., Sahling, I. and Stepochkin, I., 2021. Retrieval of the Full Complex of Optical Characteristics for Heat Content Assessing in the Southern Part of the Barents Sea in June. *Sovremennye Problemy Distantsionnogo Zondirovaniya Zemli iz Kosmosa*, 18(5), pp. 214-225. https://doi.org/10.21046/2070-7401-2021-18-5-214-225 (in Russian).

6. Korchemkina, E.N., Shybanov, E.B. and Lee, M.E., 2009. Atmospheric Correction Improvement for the Remote Sensing of Black Sea Waters. *Issledovanie Zemli iz Kosmosa*, (6), pp. 24-30 (in Russian).

7. Kopelevich, O.V., Sahling, I.V., Vazyulya, S.V., Glukhovets, D.I., Sheberstov, S.V., Burenkov, V.I., Karalli, P.G. and Yushmanova, A.V., 2018. *Bio-Optical Characteristics of the Seas, Surrounding the Western Part of Russia, from Data of the Satellite Ocean Color Scanners of 1998-2017*. Moscow: OOO "Vash Format", 140 p. (in Russian).

8. Suetin, V.S., Korolev, S.N., Suslin, V.V. and Kucheryavyi, A.A., 2004. Manifestation of Specific Features of the Optical Properties of Atmospheric Aerosol over the Black Sea in the Interpretation of SeaWiFS Data. *Physical Oceanography*, 14(1), pp. 57-65. https://doi.org/10.1023/B:POCE.0000025370.99460.88

9. Suetin, V.S and Korolev, S.N., 2021. Application of Satellite Data for Retrieving the Light Absorption Characteristics in the Black Sea Waters. *Physical Oceanography*, 28(2), pp. 205-214. https://doi.org/10.22449/1573-160X-2021-2-205-214

10. Kabashnikov, V., Milinevsky, G., Chaikovsky, A., Miatselskaya, N., Danylevsky, V., Aculinin, A., Kalinskaya, D., Korchemkina, E., Bovchaliuk, A. [et al.], 2014. Localization of Aerosol Sources in East-European Region by Back-Trajectory Statistics. *International Journal of Remote Sensing*, 35(19), pp. 6993-7006. https://doi.org/10.1080/01431161.2014.960621

11. Zibordi, G., Mélin, F., Berthon, J.-F., Holben, B., Stutsker, I., Giles, D., D'Alimonte, D., Vandemark, D., Feng, H. [et al.], 2009. AERONET-OC: A Network for the Validation of Ocean Color Primary Products. *Journal of Atmospheric and Oceanic Technology*, 26(8), pp. 1634-1651. https://doi.org/10.1175/2009JTECHO654.1

12. Kalinskaya, D.V. and Suslin V.V., 2015. Simple Method of Determination of Ground-Based Aerosol Sources Using Back Trajectory Analysis Results. *Fundamental and Applied Hydrophysics*, 8(1), pp. 59-67 (in Russian).

13. Kalinskaya, D.V. and Papkova, A.S., 2022. Why Is It Important to Consider Dust Aerosol in the Sevastopol and Black Sea Region during Remote Sensing Tasks? A Case Study. *Remote Sensing*, 14(8), 1890. https://doi.org/10.3390/rs14081890

14. Wang, M., Son, S. and Harding, L.W. Jr., 2009. Retrieval of Diffuse Attenuation Coefficient in the Chesapeake Bay and Turbid Ocean Regions for Satellite Ocean Color Applications. *Journal of Geophysical Research: Oceans*, 114(C10), C10011. https://doi.org/10.1029/2009JC005286

15. Schollaert, S.E., Yoder, J.A., O'Reilly, J.E. and Westpha, D.L., 2003. Influence of Dust and Sulfate Aerosols on Ocean Color Spectra and Chlorophyll a Concentrations Derived from SeaWiFS off the U.S. East Coast. *Journal of Geophysical Research: Oceans*, 108(C6), 3191. https://doi.org/10.1029/2000JC000555

16. Suetin, V.S., Korolev, S.N. and Kucheryavy, A.A., 2014. Application of Satellite Observations for Determining Spectral Dependences of the Black Sea Waters Optical Characteristics. *Morskoy Gidrofizicheckiy Zhurnal*, (3), pp. 77-86 (in Russian).

17. Kalinskaya, D.V. and Papkova, A.S., 2023. Variability of the Water-Leaving Radiance under the Conditions of Dust Transport by the Satellite Sentinel-3 Data on the Example of the Black Sea and Sevastopol. *Physical Oceanography*, 30(3), pp. 369-383. https://doi.org/10.29039/1573-160X-2023-3-369-383

18. Shybanov, E.B. and Papkova, A.S., 2022. Differences in the Ocean Color Atmospheric Correction Algorithms for Remote Sensing Reflectance Retrievals for Different Atmospheric Conditions. *Sovremennye Problemy Distantsionnogo Zondirovaniya Zemli iz Kosmosa,* 19(6), pp. 9-17. https://doi.org/10.21046/2070-7401-2022-19-6-9-17 (in Russian).

19. Wei, X., Chang, N.-B., Bai, K. and Gao, W., 2020. Satellite Remote Sensing of Aerosol Optical Depth: Advances, Challenges, and Perspectives. *Critical Reviews in Environmental Science and Technology*, 50(16), pp. 1640-1725. https://doi.org/10.1080/10643389.2019.1665944

20. Wang, X., 2018. New Methods for Improving the Remote Sensing Estimation of Soil Organic Matter Content (SOMC) in the Ebinur Lake Wetland National Nature Reserve (ELWNNR) in Northwest China. *Remote Sensing of Environment*, 218, pp. 104-118. https://doi.org/10.1016/j.rse.2018.09.020

21. Gordon, H.R., 2021. Evolution of Ocean Color Atmospheric Correction: 1970–2005. *Remote Sensing*, 13(24), 5051. https://doi.org/10.3390/rs13245051

22. Moulin, S., Launay, M. and Guérif, M., 2001. The Crop Growth Monitoring at a Regional Scale Based on the Combination of Remote Sensing and Process-Based Models. In: K. Kobayashi, ed., 2001. *Proceedings of NIAES-STA International Workshop 2001: Crop Monitoring and Prediction at Regional Scales*. Tsukuba, Japan, pp. 187-195.

23. Korchemkina, E.N. and Kalinskaya, D.V., 2022. Algorithm of Additional Correction of Level 2 Remote Sensing Reflectance Data Using Modelling of the Optical Properties of the Black Sea Waters. *Remote Sensing*, 14(4), 831. https://doi.org/10.3390/rs14040831

24. Kopelevich, O.V., Burenkov, V.I. and Sheberstov, S.V., 2006. Development and Use of Regional Algorithms for Calculation of Bio-Optical Characteristics of Russian Seas Based on Satellite Color Scanner Data. *Sovremennye Problemy Distantsionnogo Zondirovaniya Zemli iz Kosmosa,* 3(2), pp. 99-105 (in Russian).

25. Remer, L.A., Kahn, R.A. and Koren, I., 2009. Aerosol Indirect Effects from Satellite: Skeptics vs. Optimists. *Geochimica et Cosmochimica Acta*, 73(13), supplement A1088. https://doi.org/10.1016/j.gca.2009.05.014

26. Suslin, V.V., Slabakova, V.K., Kalinskaya, D.V., Pryakhina, S.F. and Golovko, N.I., 2016. Optical Features of the Black Sea Aerosol and the Sea Water Upper Layer Based on In Situ and Satellite Measurements. *Physical Oceanography*, (1), pp. 20-32. https://doi.org/10.22449/1573-160X-2016-1-20-32

27. Gordon, H.R. and Wang, M., 1994. Influence of Oceanic Whitecaps on Atmospheric Correction of Ocean-Color Sensors. *Applied Optics*, 33(33), pp. 7754-7763. https://doi.org/10.1364/AO.33.007754

28. Glantz, P., Freud, E., Johansson, C., Noone, K.J. and Tesche, M., 2019. Trends in MODIS and AERONET Derived Aerosol Optical Thickness over Northern Europe. *Tellus B: Chemical and Physical Meteorology*, 71(1), 1445379. https://doi.org/10.1080/16000889.2018.1554414

29. Zibordi, G., Melin, F., Berthon, J.-F. and Talone, M., 2015. In Situ Autonomous Optical Radiometry Measurements for Satellite Ocean Color Validation in the Western Black Sea. *Ocean Science*, 11(2), pp. 275-286. https://doi.org/10.5194/os-11-275-2015

30. Thuillier, G., Hersé, M., Labs, D., Foujols, T., Peetermans, W., Gillotay, D., Simon, P.C. and Mandel, H., 2003. The Solar Spectral Irradiance from 200 to 2400 nm as Measured by the SOLSPEC Spectrometer from the Atlas and Eureca Missions. *Solar Physics*, 214(1-22), pp. 1-22. https://doi.org/10.1023/A:1024048429145

31. Suetin, V.S., Kucheryavyi, A.A., Suslin, V.V. and Korolev, S.N., 2000. Concentrations of Phytoplankton in the North-Western Part of the Black Sea Based on Data of Measurements by Satellite Color Scanner CZCS. *Morskoy Gidrofizicheckiy Zhurnal*, (2), pp. 74-82 (in Russian).

32. Omar, A.H., Winker, D.M., Vaughan, M.A., Hu, Y., Trepte, C.R., Ferrare, R.A., Lee, K.-P., Hostetler, C.A., Kittaka, C. [et al.], 2009. The CALIPSO Automated Aerosol Classification and Lidar Ratio Selection Algorithm. *Journal of Atmospheric and Oceanic Technology*, 26(10), pp. 1994-2014. https://doi.org/10.1175/2009JTECHA1231.1

33. Omar, A.H., Tackett, J. and Al-Dousari, A., 2022. CALIPSO Observations of Sand and Dust Storms and Comparisons of Source Types near Kuwait City. *Atmosphere,* 13(12), 1946. https://doi.org/10.3390/atmos13121946

34. Stein, A.F., Draxler, R.R., Rolph, G.D., Stunder, B.J.B., Cohen, M.D. and Ngan, F., 2015. NOAA's HYSPLIT Atmospheric Transport and Dispersion Modeling System. *Bulletin of the American Meteorological Society*, 96(12), pp. 2059-2077. https://doi.org/10.1175/BAMS-D-14-00110.1

35. Yakovleva, D.V., Tolkachenko, G.A., Kholben, B.N. and Smirnov, A.V., 2009. Seasonal and Interannual Variability of the Atmospheric Optical Characteristics over the Black Sea near Sevastopol in the Period 2006-2008. In: MHI, 2009. *Ecological Safety of Coastal and Shelf Zones and Comprehensive Use of Shelf Resources*. Sevastopol: ECOSI-Gidrofizika. Iss. 18, pp. 205-212 (in Russian).

36. Werdell, P.J. and Bailey, S.W., 2002. The *SeaWiFS Bio-Optical Archive and Storage System (SeaBASS): Current Architecture and Implementation*. NASA/TM 2002–211617. Greenbelt, MD, USA: Goddard Space Flight Center, 45 p.

About the authors:

Anna S. Papkova, Junior Researcher, Marine Hydrophysical Institute of RAS (2 Kapitanskaya Str., Sevastopol, 299011, Russian Federation), CSc. (Phys.-Math.), **Scopus Author ID: 57203015832**, hanna.papkova@gmail.com

Evgeniy B. Shybanov, Leading Researcher, Marine Hydrophysical Institute of RAS (2 Kapitanskaya Str., Sevastopol, 299011, Russian Federation), DSc. (Phys.-Math.), **Scopus Author ID: 6507075380**, **WoS ResearcherID: ABB-9097-2021**, e-shybanov@mail.ru

Darya V. Kalinskaya, Junior Researcher, Marine Hydrophysical Institute of RAS (2 Kapitanskaya Str., Sevastopol, 299011, Russian Federation), **Scopus Author ID: 56380591500**, kalinskaya@mhi-ras.ru

Contribution of the co-authors:

Anna S. Papkova – conceptualization, methodology, investigation, data collection, visualization and curation, preparatory drafting, review and editing

Evgeniy B. Shybanov – curation, methodology, investigation, formal analysis, editing

Darya V. Kalinskaya – methodology, data collection, investigation, visualization, preparatory drafting, editing

The authors have read and approved the final manuscript.
The authors declare that they have no conflict of interest.